

High-Resolution Nuclear Magnetic Resonance Spectroscopy

Advances in instrumentation in this field are leading to new applications in chemistry and biology.

R. C. Ferguson and W. D. Phillips

The bewildering pace of science since World War II is well illustrated by nuclear magnetic resonance (NMR) spectroscopy (1-3). Bloch and Purcell shared the 1952 Nobel prize in physics for their independent discoveries in 1946 of the phenomenon of nuclear magnetic resonance (4, 5). The first commercial high-resolution NMR spectrometer, operated at a proton magnetic resonance (PMR) frequency of 30 megahertz, became available in 1953 (6). The PMR frequency has since been advanced to 40 (1955), 60 (1958), 100 (1962), and 220 megahertz (1966) (6). These and other major advances in instrumentation greatly extended applicability of the technique.

The exceptional usefulness of the technique in chemistry accounts for its rapid development; along with other spectroscopic methods, NMR has revolutionized the identification and characterization of molecules, largely eliminating laborious chemical procedures. Other applications of NMR, such as elucidation of electron distributions in molecules, of molecular motions, and of exchange phenomena, have attracted the attention of physicists and biologists also.

In some respects NMR has reached

its maturity; most of the world's chemical laboratories are equipped with such spectrometers or have access to them, and the method is one of several routine analytical tools. However, the field is far from static. New advances in instrumentation, especially the development of spectrometers operating at higher frequencies and with improved stability and sensitivity, have not only increased the scope of conventional applications, but have also made possible entirely new applications. Here we shall outline some recent significant developments in chemical and biological applications.

The Resonance Phenomenon

Nuclear magnetic resonance involves the observation of radio frequency-induced transitions between quantized energy states of magnetic nuclei polarized by magnetic fields. The basic resonance condition is given by the Larmor relation $\omega = \gamma H$, where ω is the resonance frequency, γ is the nuclear magnetogyric ratio, and H is the magnetic field strength at the nucleus. The usefulness of NMR arises from the effects of inter- and intramolecular interactions on the values of H at the nuclear sites in molecules.

Of the approximately 150 isotopic species that possess permanent nuclear

magnetic moments, about 25 have been employed in chemical applications of NMR; some of the more useful nuclei are listed in Table 1. Probably more than 90 percent of all NMR work is on H^1 , with an additional 5 percent on F^{19} and P^{31} . The outstanding NMR characteristics of these nuclei (natural abundance; NMR sensitivity; spin, $\frac{1}{2}$), as well as their importance in chemistry, account for this concentration of effort. The major isotopes of some other important elements, such as C^{12} and O^{16} , have zero magnetic moment, but the resonances of the less-abundant isotopes C^{13} and O^{17} have been usefully applied (2, pp. 988-1031, 1042-48). Improvements in spectrometer sensitivity have facilitated studies of other less-abundant isotopes, and additions to the list of useful nuclei may be expected.

Instrumentation

The essential components of an NMR spectrometer are the magnet, sample probe, radio-frequency (rf) units, and accessories for recording the spectra. Chemical shifts and spectrometer sensitivity are field-dependent, so it is desirable to operate at the highest field strength for which adequate homogeneity and stability can be achieved. For high-resolution spectrometers, typical requirements for magnets operating in the 25- to 50-kilogauss range are a field homogeneity of $1:10^8$ over a volume of about 0.1 cubic centimeter and field and rf stabilities of $1:10^9$ over a period of several minutes. Formerly, iron-core electromagnets or permanent magnets were employed. The first commercial NMR spectrometer operated at 7.04 kilogauss; the PMR frequency was 30 megahertz, but with improved electromagnet systems it was increased through stages to 100 megahertz. Further significant increases in field strength have been achieved with superconducting solenoids (7), and a high-resolution NMR spectrometer operating at 51.7 kilogauss (PMR absorption at 220 megahertz) is now used in our laboratory (Fig. 1).

The sample probe contains electrical

Dr. Ferguson is a research chemist and Dr. Phillips is an associate director in the Central Research Department, E. I. du Pont de Nemours and Co., Inc., Wilmington, Delaware 19898.

Table 1. Characteristics pertinent to NMR absorption for some isotopes. Nuclear magnetic resonance frequencies are for a 23.49-kilogauss field; sensitivities are expressed relative to the same numbers of protons.

Isotope	NMR frequency (Mhz)	Sensitivity	Natural abundance (%)	Nuclear spin
H ¹	100	1.00	99.98	1/2
H ²	15.4	9.64 × 10 ⁻³	1.56 × 10 ⁻²	1
H ³	107	1.21		1/2
B ¹⁰	10.7	1.99 × 10 ⁻²	18.83	3
B ¹¹	32.1	0.165	81.17	3/2
C ¹³	25.1	1.59 × 10 ⁻²	1.108	1/2
N ¹⁴	7.2	1.01 × 10 ⁻³	99.635	1
N ¹⁵	10.1	1.04 × 10 ⁻³	0.365	1/2
O ¹⁷	13.6	2.91 × 10 ⁻²	3.7 × 10 ⁻²	5/2
F ¹⁹	94.1	0.834	100	1/2
Na ²³	26.5	9.27 × 10 ⁻²	100	3/2
P ³¹	40.5	6.64 × 10 ⁻²	100	1/2
K ³⁹	44.7	5.08 × 10 ⁻¹	93.08	3/2
Co ⁵⁹	23.7	0.281	100	7/2

coils for coupling the sample with the rf units, for sweeping the magnetic field through the resonance region, and for fine adjustments of the magnetic-field homogeneity. (The last-mentioned coils are more frequently mounted on the pole faces of iron-core magnets.) Most probes have provision for control of the temperature of the sample, which is contained in a cylindrical glass tube supported by an air-bearing turbine that spins the tube to average field gradients across the sample.

Most high-resolution NMR spectrometers employ fixed-frequency rf units for observation of resonance absorption as the magnetic-field strength is varied; some have an optional frequency-sweep mode of operation. Most modern spectrometers also have provision for electronic integration of the spectra for quantitative applications.

Of the many other improvements in design of spectrometers, better time stability is perhaps most significant. Along with field homogeneity, time stabilities of the field-frequency relation and of the field homogeneity are the limiting variables affecting resolution and sensitivity. Independent stabilization of the rf units and magnet systems is difficult, and the field-frequency relation is more reliably maintained by means of servo loops that employ the nuclear resonance line of a reference compound in the experimental sample or in a separate control sample in the probe. A final touch of sophistication is use of the resonance of the internal reference compound to stabilize the field homogeneity as well.

With well-stabilized spectrometers, the repeatability of successive spectral scans permits use of an on-line computer to further improve sensitivity. In the com-

puter-of-average-transients (CAT) technique, *n* scans of the spectrum are additively accumulated in the memory of the computer. The theoretical enhancement of signal-to-noise ratio is *n*^{1/2}; the improvement is limited only by the time stability of the spectrometer-computer system. Ten- to 50-fold improvements in sensitivity, requiring up to a few hours of stable operation, are now fairly routine.

Improvements in sensitivity were initially sought for the study of small samples (in the microliter range) and for compounds of low solubility. However, one of the greatest current benefits is in the examination of nuclei that are of low natural abundance or low intrinsic signal strength. Some new spectrometers can accumulate spectra in an on-line computer for 24 to 36 hours; sensitivity is adequate to produce high-quality C¹³ spectra at the natural abundance level and to obtain N¹⁵ spectra on isotopically enriched samples (8).

Spectra and Molecular Structure

The parameters that describe nuclear spin systems are the chemical shifts (δ_i), the nuclear spin-spin coupling constants (J_{ij}), and the spin-lattice (T_1) and spin-spin (T_2) relaxation times of the nuclei; all depend on molecular structure and molecular motions. In solids, direct magnetic dipole-dipole interactions dominate, the relaxation times are short, and the NMR spectra consist of very broad lines. In liquids and gases, the direct dipole-dipole interactions usually are averaged to zero by rapid intra- and intermolecular motions, the relaxation

times are much longer, and narrow-line NMR spectra are observed. For most purposes, high-resolution NMR spectra are describable in terms of chemical shifts and coupling constants. Internal rotation, chemical exchange, and other rate processes can, however, affect relaxation times so as to produce pronounced, temperature-dependent effects on the spectra. Utilization of these effects in the study of dynamic processes of molecules is another important application of NMR (2, pp. 481-588; 3, pp. 218-30, 365-99; 9).

Chemical shifts arise from partial shielding of the nuclei from the applied magnetic field by the electrons surrounding the nuclei. Chemical shifts are field-dependent and characteristic of the local structural environments of the nuclei. Spin-spin coupling constants are field-independent magnetic interactions transmitted between nuclei in the molecule by the bonding and nonbonding electrons. These spin-spin interactions split the chemically shifted resonances into multiplets. Coupling constants are usually largest for directly bonded nuclei and decrease rapidly as the number of intervening bonds increases; therefore they provide additional information about the arrangements of atoms in the molecule.

The resonance frequencies and intensities of high-resolution NMR spectra can be calculated by standard quantum-mechanical procedures, employing the Hamiltonian operator

$$H = \frac{1}{2\pi} \sum_i \gamma_i H_0 (1 - \sigma_i) I_{zi} + \sum_{i < j} J_{ij} I_i \cdot I_j \quad (1)$$

for the steady-state nuclear-spin energies. Here γ_i is the magnetogyric ratio of the *i*th nucleus, σ_i is its screening constant, I_i is its angular momentum operator having the projection I_{zi} on the axis of the applied magnetic field H_0 , and J_{ij} is the coupling constant between nuclei *i* and *j*.

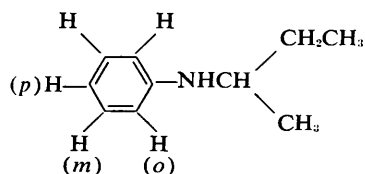
Theoretical calculation of screening constants and coupling constants is possible only for very simple molecules. Application of NMR to structure analysis, therefore, is based primarily on empirical correlation of structure with observed chemical shifts (which are linear functions of the screening constants) and coupling constants. Nuclear magnetic resonance spectra usually are calibrated with respect to the resonance of a reference compound. The chemical shift of the *i*th nucleus is defined as

$$\delta_i = 10^{-6}(H_i - H_r)/H_r = 10^{-6}(\nu_r - \nu_i)/\nu_r$$

and is expressed in parts per million. Here H is the magnetic-field strength for resonance at constant frequency, and ν is the resonance frequency at constant field strength; the subscripts refer, respectively, to the i th and reference nuclei. The coupling constants are always expressed in frequency units (hertz).

If $|\nu_i - \nu_j| \gg J_{ij}$ for all sets of non-equivalent nuclei, the NMR spectrum is usually simple and is termed first-order. In this situation chemical shifts and coupling constants can be deduced directly from the spectrum. When $|\nu_i - \nu_j|$ and J_{ij} are comparable in magnitude, the spectrum may be quite complicated, and approximation methods or computer calculations that employ the Hamiltonian operator of Eq. 1 may be required to extract the NMR parameters.

The 60- and 220-megahertz PMR spectra of *N*-*sec*-butyl aniline (Fig. 2)



illustrate the sensitivity of high-resolution NMR spectra to structure, and the advantages of operating at the highest-possible frequency. The 60-megahertz spectrum is a perturbed first-order spectrum, with some confusing overlap of resonances. The 220-megahertz spectrum is almost completely first-order. The resonances are readily assignable to protons or groups of equivalent protons having chemical shifts, in parts per million, of 7.05 (*m*), 6.58 (*p*), 6.39 (*o*), 3.37 (NH), 3.12 (CH), 1.27 (CH₂), 0.92 (CH₃), and 0.77 (CH₃). The relative intensity of each of the multiplets is proportional to the number of protons in the group. The line spacings in each multiplet are equal to the coupling constants, and the number of lines in the multiplet is $n + 1$, where n is the number of nuclei producing the splitting. Thus the doublet at 0.92 part per million is due to the CH₃ group attached to the CH group, and the triplet at 0.77 part per million is due to the CH₃ group attached to the CH₂ group. Except for the CH₂ multiplet, all can also be analyzed by first-order coupling considerations.

Detailed analyses of the NMR spectra of many compounds have established that chemical shifts and coupling constants are highly characteristic and to a large extent independent of the other groups present in a molecule. Extensive

structure-parameter correlations provide a basis for interpretation of the spectra and for establishment of the structures of compounds (2, vol. 2). One of the unique advantages of NMR, moreover, is that spectra can often be interpreted without reference to data from structurally related compounds; this feature is particularly important in the study of new compounds of unusual structure.

Chemical Shifts and

Spin-Spin Couplings

Although the origins of chemical shifts and coupling constants are understood rather well in a formal sense, and rigorous quantum-mechanical descriptions of the phenomena have been developed (2, pp. 59-200; 3, pp. 165-

98), quantitative agreement between theoretically and experimentally derived parameters is the exception rather than the rule. Explicit solutions of the quantum-mechanical problems require molecular-orbital or valence-bond wave functions which usually are inadequate approximations for calculation of NMR parameters. Nevertheless, theoretical treatments have yielded several useful qualitative and semiquantitative predictions of the relations between structure and NMR parameters. Situations in which one factor or effect dominates have yielded the most useful theoretical results, as in the following examples.

The effect of an external magnetic field on an aromatic ring system, such as benzene, can be described in terms of an induced circulation of the delocalized π -electrons that produces aniso-

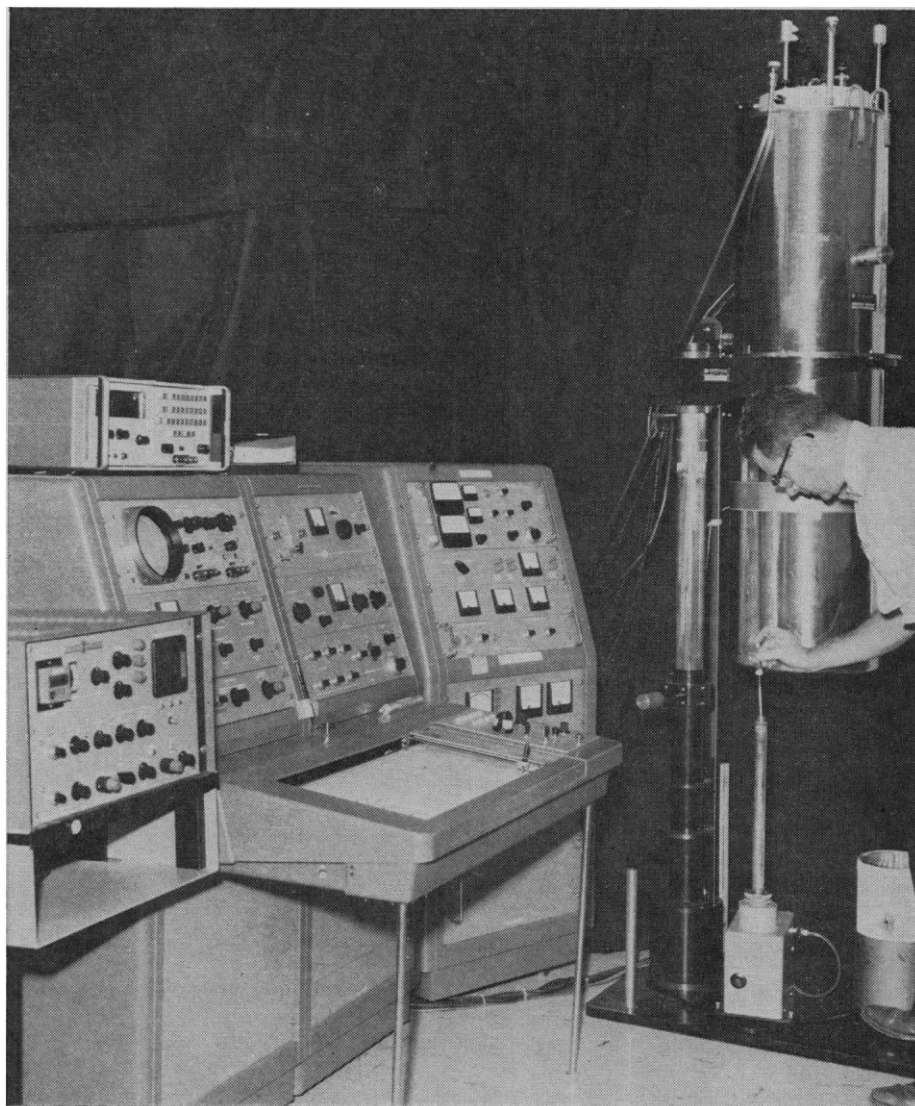


Fig. 1. The Varian HRSC-1X superconducting-solenoid NMR system. One of us (R.C.F.) is inserting a sample into the probe. The probe assembly is rotated and raised for insertion of the probe barrel into the room-temperature bore of the solenoid cryostat (behind his head). Other major components are (right to left) the solenoid power supply, the spectrometer console, and the C-1024 time-averaging computer.

tropic local fields. These fields either add to or subtract from the external polarizing field (10). This ring-current model (Fig. 3) has accounted for many chemical shift phenomena where aromatic systems were involved; important examples are found in the PMR spectra of the porphyrins (11), such as deu-

teroporphyrin IX (Fig. 4). The methine protons (α , β , γ , δ) exhibit resonance at an anomalously low field that, however, is consistent with their in-plane positions exterior to the ring, where the field resulting from the ring current reinforces the external field. The NH protons are located inside the porphyrin

ring, where the ring-current field should oppose the external field; and indeed the NH resonance occurs several parts per million to high field of its normal position.

An important contribution to the chemical shift, especially for nuclei other than protons, arises from the mixing of ground and excited electronic states of the molecule. An especially interesting series in which this term dominates was found in the Co^{59} resonances of octahedrally coordinated Co(III) . Theory indicated that, if this "paramagnetic" term dominated, the Co^{59} chemical shift should be linear function of the longest wavelength of electronic absorption in these complexes (12); Fig. 5 shows this prediction to be verified (13).

Nuclear magnetic resonance can provide useful information about structure and electron distributions for certain paramagnetic chelates and coordination compounds of the transition metals. Delocalization of electrons from the transition metal to the ligand groups by way of metal-ligand σ - or π -bonding is the dominating effect in these instances. For example, in Ni(II) N,N' -bis-(*p*-1,3-butadienylphenyl) aminotroponeimineate (Fig. 6) there is a partial delocalization of the two unpaired electrons of nickel into the π -electron system of the aminotroponeimine ligand. The resonances of the protons of the ligand, instead of being spread over a range of about 100 hertz as in the diamagnetic zinc chelate, extend over a range of about 6,700 hertz (Fig. 6). The large displacements of the resonances, called isotropic hyperfine contact interaction shifts, are attributable to unpaired electron spin density in the $p\pi$ -orbitals of the carbon atoms to which the protons are attached; carbon $p\pi$ -spin densities can be estimated from the NMR contact shifts (14). Electron distributions in many organic ligands, and details of metal-ligand bonding have been elucidated by this approach (15). Contact shifts have also been employed to study electron-transfer reactions (16) and ion-pair formation in solution (17). Kowalsky has observed in the PMR spectrum of cytochrome-*c* large contact shifts (18) whose interpretation may lead to deeper understanding of structure and electron transport in paramagnetic molecules of biological significance.

The nucleus-electron hyperfine contact interaction also makes a major contribution to nuclear spin-spin coupling, especially between directly bonded nuclei. For hydrocarbons, theory predicts that the contact contribution to the

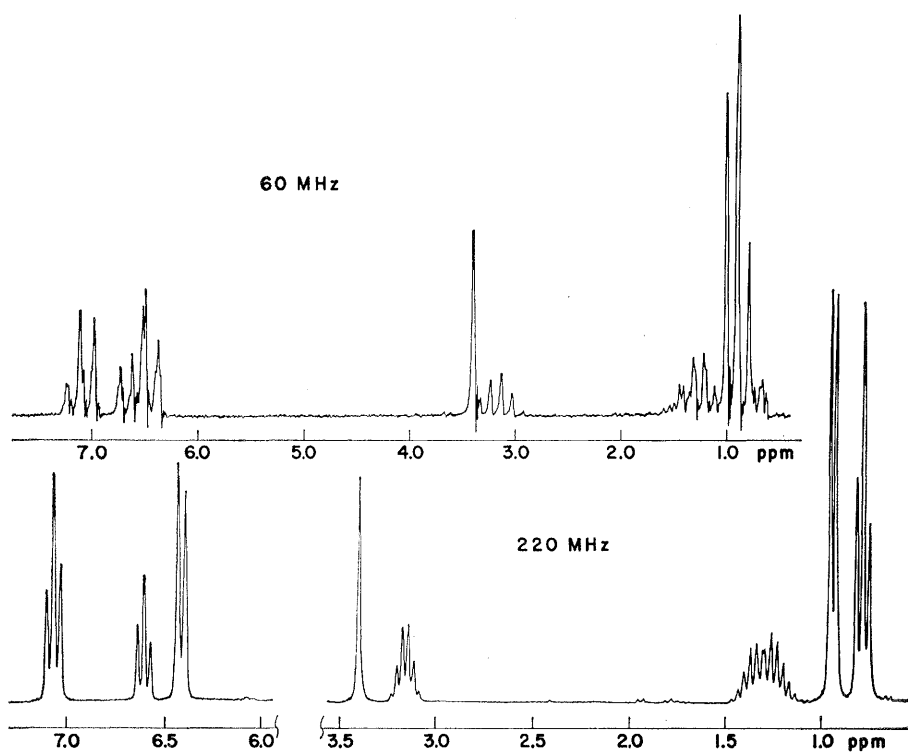


Fig. 2. Proton magnetic resonance spectra of *N-sec*-butyl aniline. The internal reference, tetramethylsilane, is here assigned a chemical shift of zero (δ -scale); another frequently used convention is the τ -scale, in which $\tau = 10 - \delta$.

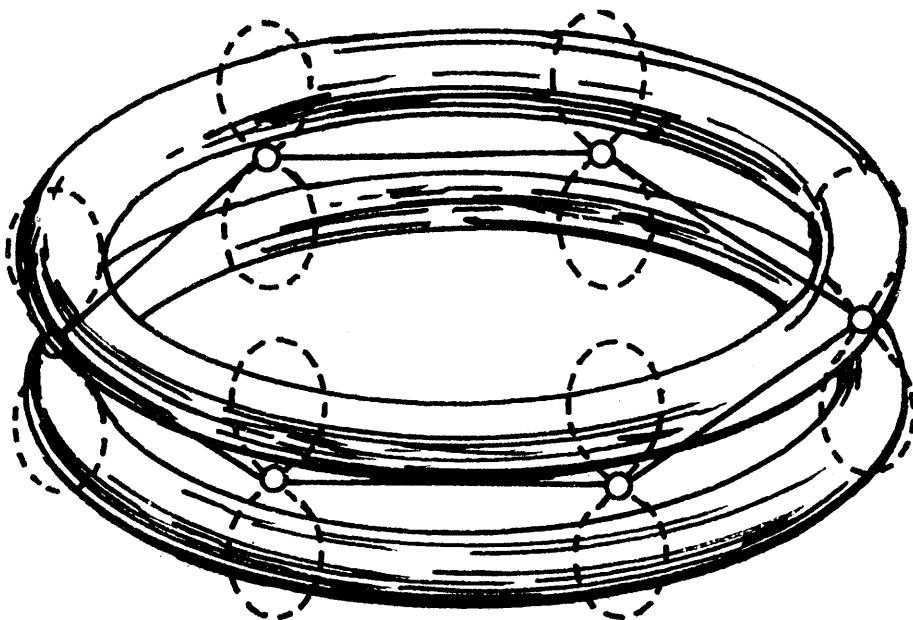


Fig. 3. Ring-current model for benzene. The six $p\pi$ -orbitals centered on carbon are indicated by the figures of eight. The delocalized circulation of the π -electrons is depicted by rings above and below the plane of the hexagon.

C^{13} — H^1 spin-spin coupling should depend on the s -characters of the carbon orbitals binding the protons. Thus C^{13} — H^1 coupling constants in methane, ethylene, and acetylene should vary

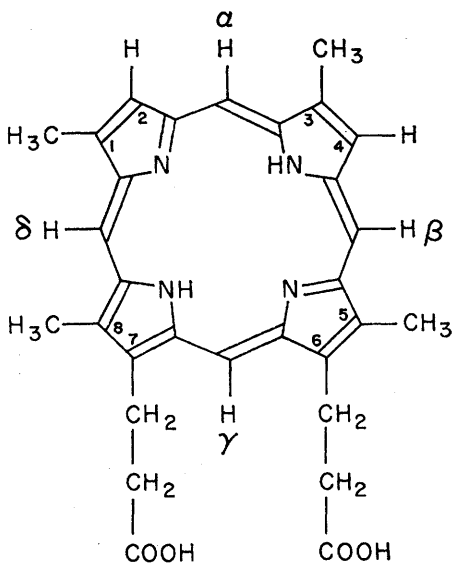


Fig. 4. Deuterioporphyrin IX.

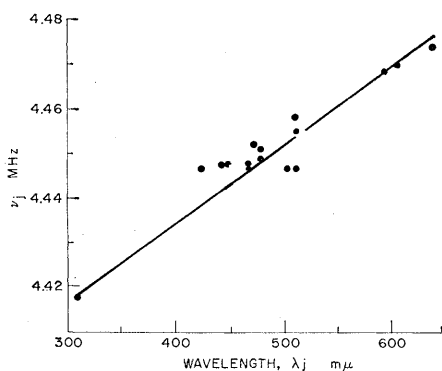
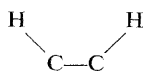


Fig. 5. The dependence of Co^{59} chemical shifts on the crystal field splitting in some octahedrally coordinated $Co(III)$ complexes. The crystal field splitting is here reflected in the longest wavelength electronic absorption. [From Freeman *et al.* (13)]

linearly with the squares of the s -characters of the hybrid bonding orbitals of carbon. These orbitals are sp^3 for methane, sp^2 for ethylene and benzene, and sp for acetylene, and the corresponding squared s -characters are, respectively, $1/4$, $1/3$, and $1/2$. Agreement between theory and experiment for this series is excellent (19).

For nuclei not directly bonded, nuclear spin-spin coupling strongly depends on bond angles. This fact is perhaps best illustrated for the case of ethane, where the coupling between protons across the C—C bond is a function of the dihedral angle in the



bond system. Karplus utilized valence-bond functions to calculate the theoretical dependence of the H^1 — H^1 coupling on the dihedral angle (Fig. 7) (20). This relation has been employed extensively in conformational analyses of cyclic and highly hindered open-chain compounds.

Ordering in Liquid Crystalline Matrices

In principle, the more quantitative aspects of molecular geometry are derivable from direct nuclear dipole-dipole interactions, which are usually larger by orders of magnitude than chemical shift and spin-spin coupling effects. For example, instead of a single resonance, the PMR spectrum of oriented H_2O molecules would be a doublet with a peak-to-peak separation of

$$\Delta H = (3\mu^2/r^3)(3\cos^2\theta - 1) \quad (2)$$

where μ is the proton nuclear-magnetic moment, r is the proton-proton internuclear distance, and θ is the angle between r and the external magnetic

field. Nuclear dipole-dipole splittings have been employed to obtain internuclear distances and angles in some solid organic and inorganic systems. An important application concerned the orientation of water molecules in hydrated collagen; the intramolecular dipole-dipole interaction of the protons of water was used as the probe (21). The method, however, has proved to be of limited utility because of the complexities of dipole-dipole splitting patterns that are encountered for systems more complicated than two-spin systems, and because of severe line-broadening effects that accompany intermolecular dipole-dipole interactions in the solid.

Dipole-dipole splittings are usually averaged to zero by the rapid tumbling motion of the molecules in liquids or solutions. (This averaging of dipole-dipole interactions is, of course, what makes high-resolution NMR spectroscopy possible.) Saupe and Englert showed, however, that the phenomenon of nuclear dipole-dipole splitting could be combined with the orientation properties of liquid crystalline systems to produce an important new approach to the geometry of molecules (22).

Certain compounds exhibit, over a well-defined temperature range, characteristics that have been described as liquid crystalline; such materials exist in one or more phase modifications consisting of one-dimensionally (nematic) or two-dimensionally (smectic) ordered arrays of molecules. The swarms or arrays of a nematic-phase system can be appreciably aligned (more than 75 percent in some instances) by magnetic fields of only a few thousand gauss. Because of this ordering effect, nematic-phase compounds give rise to widely split dipole-dipole multiplets even though they exhibit a viscosity approaching that of a normal isotropic liquid. Nematic systems may be em-

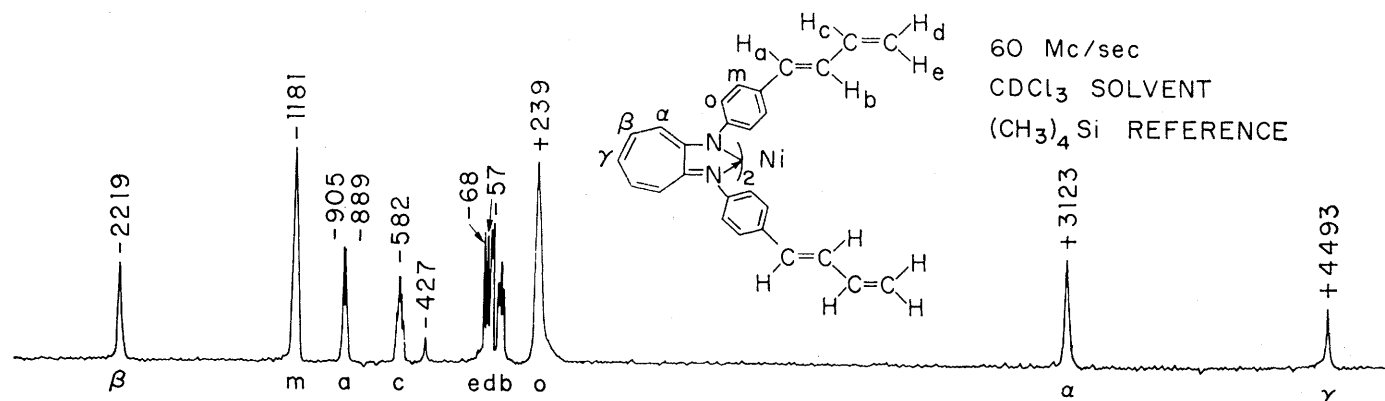


Fig. 6. A 60-megahertz PMR spectrum of $Ni(II)$ N,N' -bis-(p -1,3-butadienyl)phenylaminotroponeimineate. Solvent, $CDCl_3$; temperature, $25^\circ C$; internal reference, tetramethylsilane. [From Eaton and Phillips (15)]

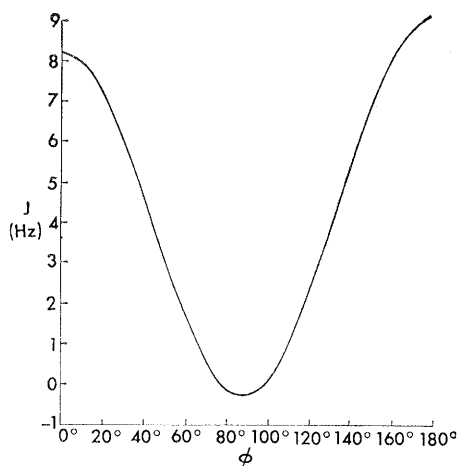
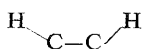


Fig. 7. Dependence of H-H spin-spin coupling, in the bond system, on angular



rotation about the C-C bond (the dihedral angle ϕ). [From Karplus (20)]

ployed as ordering solvents, and the partial orientation of the solute produced by the nematic matrix is manifested in resolved dipole-dipole splittings of a few hertz to a few kilohertz. A special virtue of this approach is that *intermolecular* dipole-dipole interactions are effectively averaged to zero by the relatively mobile liquid-crystal solution, so that the *intramolecular* dipole-dipole splittings are resolved.

The F^{19} spectrum of a solution of hexafluorobenzene in the nematogenic solvent *p*-di-*n*-hexyloxyazoxybenzene is

shown in Fig. 8 (top) (23). Since all fluorine atoms of C_6F_6 are equivalent by symmetry, the molecule should produce only a single unsplit F^{19} resonance in the absence of manifestations of dipole-dipole interactions, but in the oriented state all the spin-spin coupling constants and the nuclear dipole-dipole interactions between the *o*-, *m*-, and *p*-fluorines are observed. The observed spectrum of C_6F_6 is well reproduced by a computer-simulated spectrum (Fig. 8) that was obtained by treating the magnitudes and signs of the six spin-spin and dipole-dipole interactions as fitting parameters. Dipole-dipole interaction parameters derived in this fashion are proving to be extremely useful in determination of molecular geometry and estimation of intranuclear distances.

Synthetic Polymers

High-resolution NMR has proved useful in elucidating the structures of polymers, and in providing quantitative data for relating structure to polymerization variables and to polymer properties. Since NMR parameters are most sensitive to short-range effects, the spectra of polymers are similar to the spectra of small molecules possessing related structures. Resonances of polymers are, however, significantly broader and more difficult to resolve and interpret.

Although containing only a single

type of monomer unit, homopolymers often have distinguishably different arrangements of monomer units within the polymer chains. For example, the polymerization of chloroprene (2-chloro-1,3-butadiene) proceeds mainly by 1,4-addition; the basic repeat units are $-\text{CH}_2\text{CCl}=\text{CHCH}_2-$, with the *trans*:*cis* ratio ordinarily being about 10. Three different arrangements of pairs of repeat units are possible:



The CH_2 resonances of the head-to-tail, head-to-head, and tail-to-tail pairs of polychloroprene are found at 2.35, 2.50, and 2.20 parts per million (Fig. 9). The relative frequencies of occurrence of these pair arrangements are readily determined by measurements of intensities at 220 megahertz, but with difficulty at 60 megahertz (24).

Nuclear magnetic resonance is unquestionably the best and sometimes the only method for determining the stereoregularity (tacticity) of vinyl polymers and other polymers possessing asymmetric centers in the polymer chain. Bovey and Tiers (25) found that two-monomer (dyad) and three-monomer (triad) tactic placement effects could be observed in the 40-megahertz spectra of poly(α -methyl methacrylate) (PMMA);

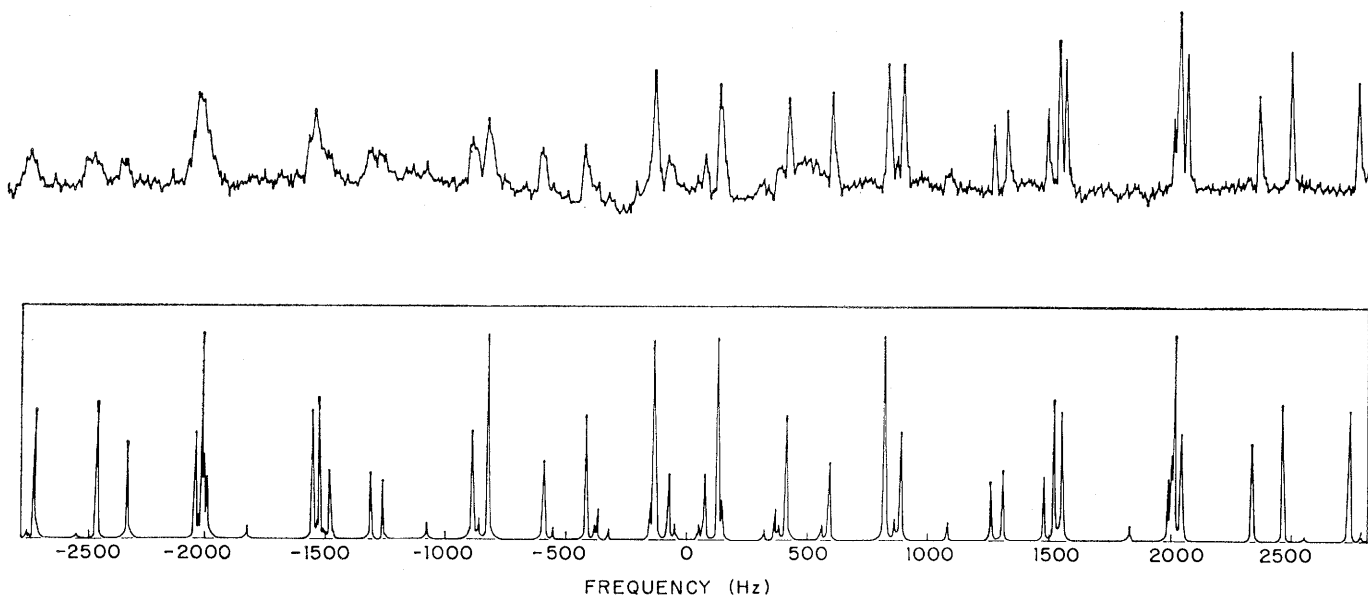
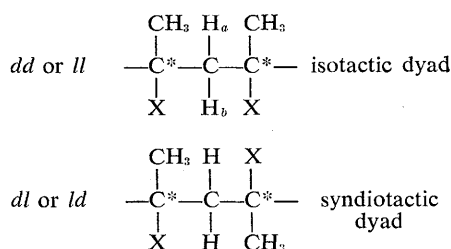


Fig. 8. (Top) A 60-megahertz F^{19} spectrum of a 40-mole percent solution of hexafluorobenzene in *p*-di-*n*-hexyloxyazoxybenzene. (Bottom) A computer simulation in which the six spin-spin couplings and dipole-dipole interactions were used as fitting parameters. [From Snyder and Anderson (23)]

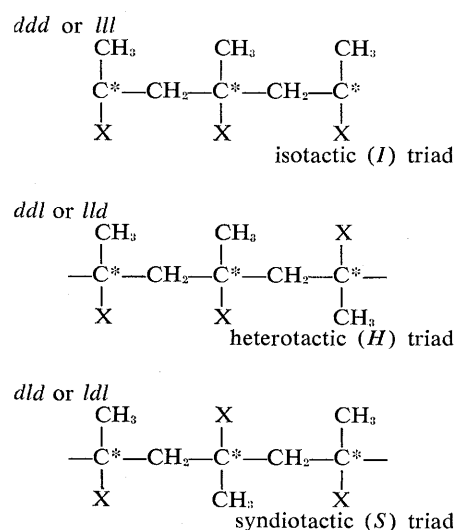
in 220-megahertz spectra of PMMA one can resolve tetrad effects and detect pentad effects.

In PMMA the CH_2 resonances are affected by the relative optical configurations of the adjacent asymmetrically substituted carbon atoms. Possible nearest-neighbor environments of CH_2 groups are



where $\text{X} = \text{COOCH}_3$ and the asterisk indicates asymmetric centers. In the isotactic dyad, the environments of protons H_a and H_b are nonequivalent, and their chemical shifts consequently differ. The PMR of such CH_2 groups consist of four peaks (a so-called AB -pattern). In the syndiotactic dyad, the chemical shifts of the two CH_2 protons are equal and give rise to a singlet resonance. In PMMA the chemical shifts are also affected by the optical configurations about the next-adjacent asymmetric carbon atoms. There are six tetrad arrangements such that three AB -patterns and three singlets are predicted.

Resonances of the methyl groups attached to the asymmetric carbon atoms are sensitive to triad placements, of which there are three:



The chemical shifts of the central methyl groups in each of these triads are different. In the 220-megahertz

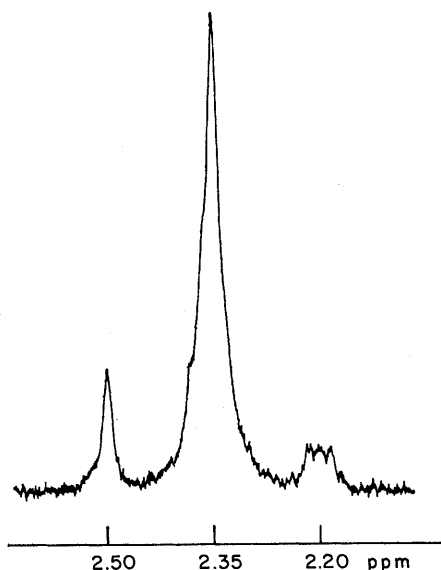


Fig. 9. A 220-megahertz PMR spectrum of polychloroprene, CH_2 region. Ten-percent solution in carbon disulfide at 40°C ; internal reference, tetramethylsilane.

spectrum of PMMA (Fig. 10), methyl triad resonances appear in the order S , H , and I at, respectively, 1.03, 1.14, and 1.27 parts per million. The line shapes and chemical shifts of these resonances are influenced slightly by the $S:H:I$ ratio, probably because of pentad placement effects. The three singlet CH_2 resonances that arise from

different tetrad arrangements appear at 1.92, 1.99, and 2.05 parts per million, respectively. The doublet resonances centered at 1.51 and 2.16 parts per million are due to two of the expected CH_2 AB -patterns, which overlap; the other tetrad arrangement occurs infrequently in this sample and its resonances are not observed.

Identification and quantitative analysis of end groups and of chain branches of polymers are other useful applications of NMR. Polyethylene, for example, is composed mainly of long-chain $(\text{CH}_2)_n$ sequences. However, at 220 megahertz the resonances of CH_3 , $-\text{CH}=\text{CH}_2$, $>\text{C}=\text{CH}_2$, and $-\text{CH}=\text{CH}-$ groups that occur as chain ends and branches can be measured quantitatively at their typical concentration levels of 0.01 to 1 percent. The improved resolution and higher sensitivity of high-frequency spectrometers, and enhancement of signal-to-noise ratio by the CAT technique, significantly increase the applicability of NMR to end- and branch-group analyses of polymers.

The monomer ratios in copolymers often can be determined most conveniently and reliably by NMR. Moreover, the relative frequencies of various arrangements of monomer sequences can be determined and employed to provide

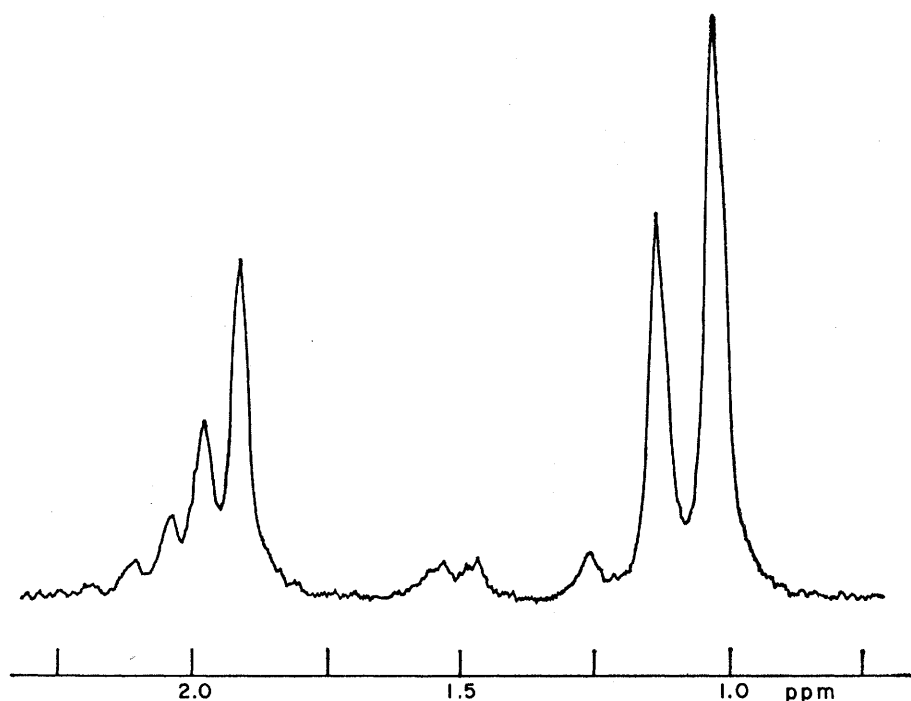


Fig. 10. A 220-megahertz PMR spectrum of poly(α -methyl methacrylate); CH_2 and $\alpha\text{-CH}_3$ regions. Ten-percent solution in *o*-dichlorobenzene at 165°C ; internal reference, hexamethyldisiloxane.

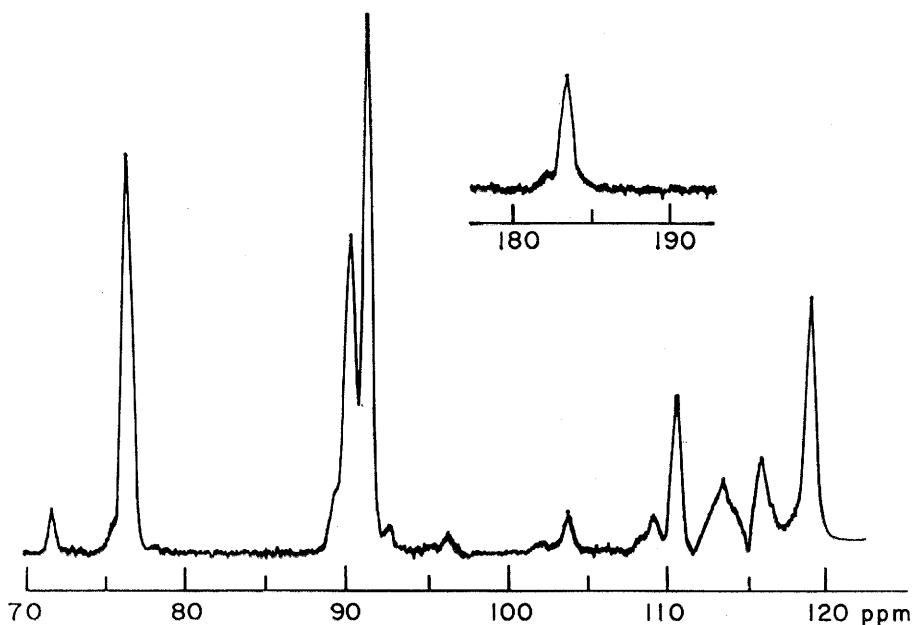


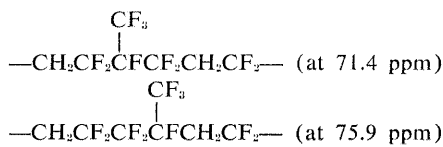
Fig. 11. A 94.1-megahertz F^{19} spectrum of a vinylidene fluoride-hexafluoropropylene copolymer at 100°C . External reference, trichlorofluoromethane.

better understanding of polymerization processes and polymer properties. The F^{19} spectra of vinylidene fluoride-hexafluoropropylene copolymers, and of other fluorine-containing polymers, have proved more useful than their H^1 spectra because of the large chemical shifts of fluorine resonances (approximately 10 times greater than proton shifts). Poly($\text{CH}_2=\text{CF}_2/\text{CF}_2=\text{CF}_2$) is a linear polymer having many different arrangements of $-\text{CH}_2\text{CF}_2-$ and



units. In the F^{19} spectra of this polymer the CF_3 , CF_2 , and CF resonances fall in the ranges 70 to 80, 90 to 120, and

180 to 185 parts per million, respectively (Fig. 11). The monomer ratio can be calculated readily from the (total CF_3):(total CF_2) intensity ratio. The CF_3 resonances are due to the comonomer arrangements



These two arrangements also produce two CF resonances. The strongest resonance of poly($\text{CH}_2=\text{CH}_2$) appears at 91.9 parts per million and is characteristic of head-to-tail vinylidene fluoride sequences; additional CF_2 resonances

appearing at 95.7, 114.0, and 116.3 parts per million arise from sequences containing head-to-head and tail-to-tail pairs (26). The corresponding resonances in Fig. 11 are split into more-complicated patterns by chemical shift differences due to the presence of hexafluoropropylene. Various other arrangements of comonomer sequences are responsible for the remaining CF_2 resonances. The relative intensities of the resonances depend on the monomer ratio and on the relative frequencies of occurrence of different five-monomer unit sequences.

The sensitivity of NMR to conformations about single bonds provides a promising approach to the study of conformations of linear macromolecules in solution. From NMR spectra of polystyrene and model compounds, Bovey *et al.* (27) have concluded that the preferred local conformation of isotactic polystyrene is helical. Since NMR is sensitive only to time-averaged local conformations, further developments in theoretical analysis of polymer spectra and the relation of local polymer conformations to other measurable properties are desirable.

Nuclear Magnetic Resonance of Biopolymers

An outstanding need in modern biology is for a physical approach that will provide information about structure and interactions at multiple atomic sites of proteins in aqueous solution. Nuclear magnetic resonance can in principle distinguish the component amino acids of proteins on the basis of side-chain proton chemical shifts. The

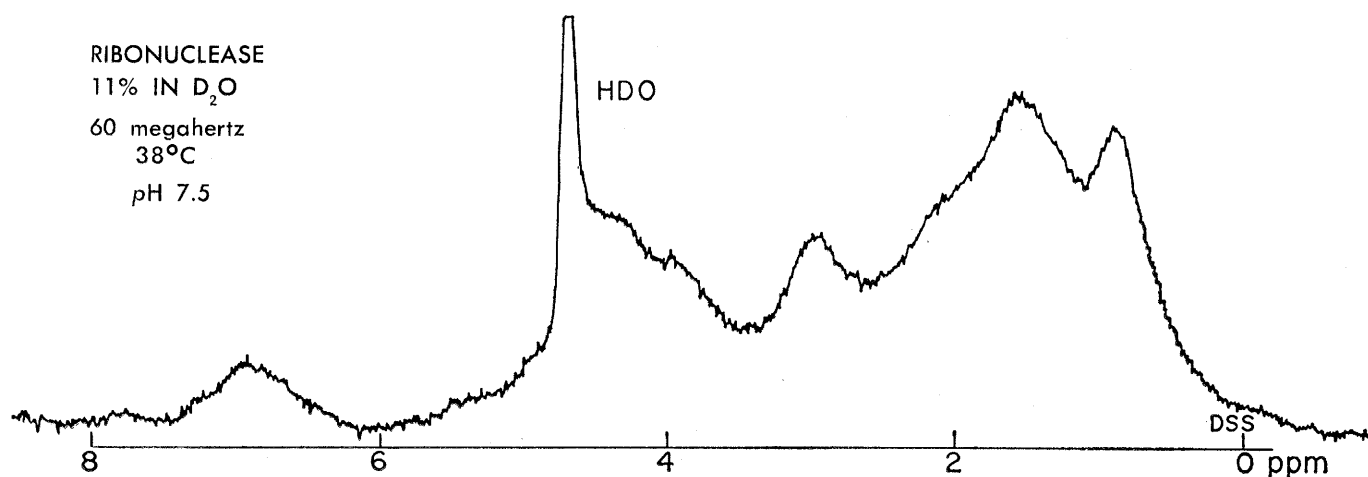


Fig. 12. A 60-megahertz PMR spectrum of an 11-percent solution of ribonuclease in D_2O .

many near-equivalences of the side-chain protons of the 20 different component amino acids lead, however, to severe overlap of their resonances. The 60-megahertz PMR spectrum of ribonuclease (Fig. 12), for example, is a virtual continuum. The factor of 11:3 enhancement in chemical shift, realized by increase of the PMR frequency from 60 to 220 megahertz (Fig. 13), is sufficient to produce spectra that are more adequate for elucidation of aspects of structure and interaction of proteins. Indeed the improvement in resolution of protein spectra at 220 megahertz is so dramatic that it compels one to contemplate the possibilities in PMR spectra of proteins at even-higher frequencies.

Manifestations, in PMR absorption, of the conformational changes that accompany protein denaturation are illustrated in the temperature dependences of the PMR spectra of ribonuclease (Fig. 13) and lysozyme (Fig. 14) (28). The PMR spectrum of ribonuclease at 22°C (below its denaturation temperature of 65°C) is markedly different from that at 72.5°C (Fig. 13). In the denatured or random-coil form, all component amino acids give rise to resonances that are essentially those of the free amino acid; the spectrum of the denatured form of the protein is very much that of a superposition of the resonances of the component amino acids, weighted by the amino acid composition of the protein. In the random-coil form, the side chains of component amino acids are largely unconstrained and exhibit chemical shifts that do not strongly reflect the amino acid sequence of the protein. In other words, in the random-coil form, nearest-neighbor interactions and conformational proximity effects do not appear to play a major role in determining the chemical shifts of the side-chain protons.

In the native form of the protein, many new resonances appear and the intensity distribution of resonances over the spectrum is markedly altered (compare the 22° and 72.5°C spectra of Fig. 13). Side-chain mobility seems to be greatly constrained in the native conformation and most of the side chains are closer together or at least more environmentally perturbed than in the random-coil form. Consequently, in the folded conformation, electrical and magnetic effects of short-range nature can produce quite appreciable chemical shifts, and the resonances of each amino acid reflect its local environment.

For illustration: the resonance absorption by the aromatic moieties of histidine, phenylalanine, and tyrosine of ribonuclease in the denatured form (the 6.8 to 7.8 parts-per-million region of the 72.5°C spectrum, Fig. 13) can be analyzed in straightforward fashion. In contrast, the various shielding environments experienced by the side chains of the aromatic residues in the native (folded) conformation of the protein are reflected in the appearance of multiple rather than single peaks for each chemically nonequivalent proton. Spectral coincidences among the four histidine residues of ribonuclease are at least partially removed in the folded conformation, as are coincidences among the six tyrosine residues and among the three phenylalanine residues.

An especially revealing manifestation of tertiary structure in proteins is seen

in the high-field resonances of lysozyme that appear in the +1 to -1 part-per-million region of the spectrum *only* in the folded form of the molecule (Fig. 14). These resonances reversibly disappear as the enzyme is denatured either thermally or by classical denaturants such as guanidine or urea. These high-field resonances are attributable to ring-current shifts induced in side-chain protons of amino acids that are forced close to the faces of the aromatic rings of the histidine, tyrosine, phenylalanine, and tryptophan residues in the protein's native conformation. High-field ring-current shifts qualitatively similar to those observed in lysozyme appear as well in the PMR spectra of the folded conformations of cytochrome-*c*, myoglobin, and hemoglobin. Additionally, in these heme proteins shifts of up to 4 parts per million are attributable to

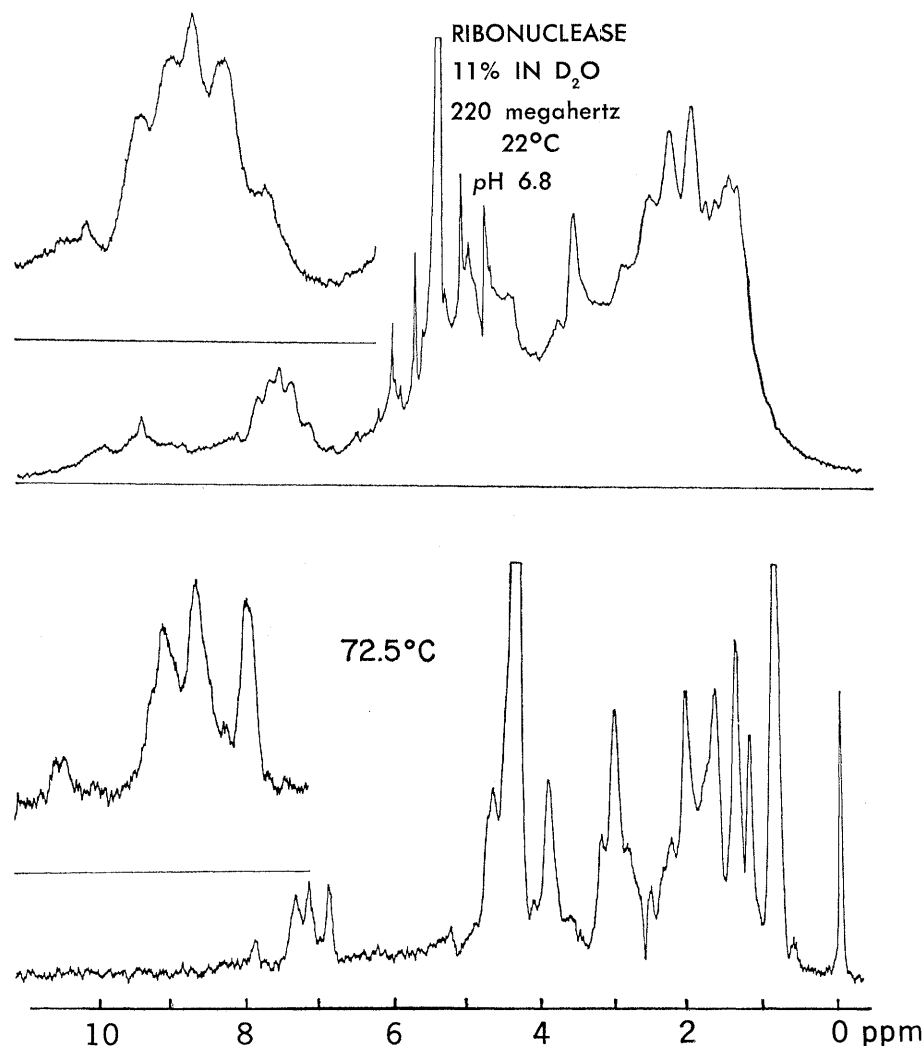


Fig. 13. Proton magnetic resonance spectra (220 megahertz) of ribonuclease in its native (folded) conformation (top) and of thermally denatured ribonuclease (bottom). Insets are expanded versions of the 6.8 to 7.8 parts-per-million region of resonance absorption. The resonance at 0 part per million arises from the internal reference sodium 2,2-dimethyl-2-silapentane-5-sulfonate.

proximity of residue side chains to the very large ring-current fields of the extended π -electron system of the porphyrin ring.

In other studies, perturbations of the PMR spectra of cofactors (29), substrates, and inhibitors (30) complexed to enzymes have been observed, and substrate-induced conformational changes in enzymes have been detected. Aggregation of protein subunits into oligomers and polymers is, incidentally, reflected in PMR line widths. It appears that high-frequency PMR spectroscopy will become a most fruitful approach to elucidation of the structures and interactions of proteins in solution.

The relatively few nonequivalent protons in nucleic acids (in contrast to proteins), and their fairly uniform distribution into "aromatic" and "saturated" types, have resulted in more successful applications of 60-megahertz PMR to nucleic acids than to proteins. Nevertheless, at 220 megahertz, PMR spectra of nucleic acids also are greatly improved, and a recent application to DNA illustrates the type of information to be derived. The two extreme high-field resonances that are observed at 220 megahertz for thermally denatured DNA are assignable to the methyl protons of the component thymine nucleosides. The relative intensities of the two methyl resonances of thymine in DNA are species-specific and have been shown (31) to reflect directly the thymine nearest-neighbor base ratio ($ApT + GpT$):($CpT + TpT$), A , G , T , C , and p being, respectively, adenine, guanine, thymine, cytosine, and phosphate. Detailed analyses of other regions of the high-frequency PMR spectra of nucleic acids can be expected to yield much more information regarding structure in this important class of compounds.

Summary

The rapid development of NMR spectroscopy has been characterized by a succession of discrete, significant advances in instrumentation, as well as by less dramatic but cumulatively important improvements in instrument performance, experimental techniques, spectral analysis, and theory. Most significant are the advances in magnet technology, which within 13 years increased the available field strengths from 7.04 to 51.7 kilogauss (with corresponding increase in the PMR frequency from 30 to 220 megahertz).

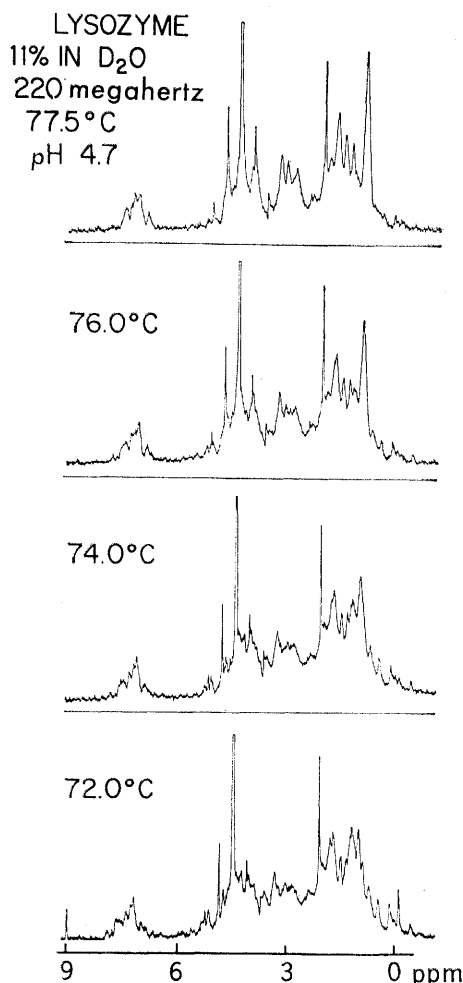


Fig. 14. Four 220-megahertz PMR spectra of lysozyme in D_2O .

Great improvements in spectrometer stability and in the coupling of spectrometers with on-line computers have so improved sensitivity that some nuclei possessing less favorable NMR characteristics can now be studied.

While initially applicable only to relatively simple molecular systems, high-resolution NMR is now being used effectively in studies of such large and structurally complex molecules as steroids and other natural products, synthetic polymers, proteins, and nucleic acids. Characterization of molecular structure continues to be the "bread and butter" application. Available methods for analysis and interpretation of spectra are highly satisfactory whenever nuclear relaxation effects can be neglected; spectral fitting methods based on the time-independent Hamiltonian operator yield accurate values for the chemical shifts and coupling constants. Although empirical correlation of these NMR parameters with structure has far outpaced quantitative theoretical treat-

ments, useful contributions to NMR are being made by quantum chemistry, and vice versa.

Nuclear magnetic resonance has been applied extensively to molecular rate processes, but quantitative treatments of spectra in terms of kinetic parameters have been possible only for very simple cases. However, the development of digital-computer methods based on time-dependent Hamiltonian operators (including nuclear relaxation times) is in progress; since many types of chemically important rate processes can be studied by NMR, these applications will become increasingly useful. In this area also, spin-echo NMR techniques will be employed extensively (32).

The development of superconducting solenoids for high-resolution NMR at frequencies of 220 megahertz and higher offers bright promise for further advances. The most significant contributions of high-frequency PMR spectroscopy will probably be in the study of biopolymers and synthetic polymers. Elucidation of structures and interactions of nucleic acids and proteins in solution promise a much better understanding of the highly specific biological functions of these complex molecules. Similarly, more detailed knowledge of the structures of synthetic polymers is important in control of their end-use properties in fibers, films, and molded products.

Other applications of NMR, only a few of which have been mentioned, are more readily accomplished with improved modern instrumentation, and increased use of NMR is to be expected.

References and Notes

1. A. Abragam, *The Principles of Nuclear Magnetism* (Clarendon Press, Oxford, 1961); N. S. Bhacca, L. F. Johnson, J. N. Shoolery, *NMR Spectra Catalog* (National Press, New York, 1962-63); N. S. Bhacca and D. H. Williams, *Applications of NMR Spectroscopy in Organic Chemistry* (Holden-Day, San Francisco, 1964); N. Bloembergen, *Nuclear Magnetic Relaxation* (Benjamin, New York, 1961); P. L. Corio *Chem. Rev.* **60**, 363 (1960); *Structure of High Resolution Nuclear Magnetic Resonance Spectra* (Academic Press, New York, 1966); H. H. Hershenson, *Nuclear Magnetic Resonance and Electron Spin Resonance Spectra, Index for 1958-1963* (Academic Press, New York, 1965); G. M. Howell, A. S. Kende, J. S. Webb, Eds., *Formula Index to NMR Literature, Vol. 1: References Prior to 1961; Vol. 2: 1961-1962 References* (Plenum, New York, 1965-66); L. M. Jackman, *Applications of Nuclear Magnetic Resonance Spectroscopy in Organic Chemistry* (Pergamon, London, 1959); J. D. Roberts, *Nuclear Magnetic Resonance* (McGraw-Hill, New York, 1959); J. D. Roberts, *An Introduction to the Analysis of Spin-Spin Splitting in High-Resolution Nuclear Magnetic Resonance Spectra* (Benjamin, New York, 1961); C. P. Slichter, *Principles of Magnetic Resonance: With Examples from Solid State Physics* (Harper and Row, New York, 1963); K.

1. B. Wiberg and B. J. Nist, *The Interpretation of NMR Spectra* (Benjamin, New York, 1962).
2. J. W. Emsley, J. Feeney, L. H. Sutcliffe, *High Resolution Nuclear Magnetic Resonance Spectroscopy* (Pergamon, London, 1965-66).
3. J. A. Pople, W. G. Schneider, H. J. Bernstein, *High-Resolution Nuclear Magnetic Resonance* (McGraw-Hill, New York, 1959).
4. F. Bloch, W. W. Hansen, M. E. Packard, *Phys. Rev.* **69**, 127 (1946); F. Bloch, *Science* **118**, 425 (1953).
5. E. M. Purcell, H. C. Torrey, R. V. Pound, *Phys. Rev.* **69**, 37 (1946); E. M. Purcell, *Science* **118**, 431 (1953).
6. Varian Associates, Palo Alto, Calif., technical literature.
7. F. A. Nelson and H. E. Weaver, *Science* **146**, 223 (1964).
8. J. D. Roberts, personal communication.
9. A. Loewenstein and T. M. Connor, *Ber. Bunsenges. Physik. Chem.* **67**, 280 (1963).
10. J. A. Pople, *J. Chem. Phys.* **24**, 1111 (1956); C. E. Johnson, Jr., and F. A. Bovey, *ibid.* **29**, 1012 (1958).
11. E. D. Becker and R. B. Bradley, *ibid.* **31**, 1413 (1959); W. S. Caughey and W. S. Koski, *Biochemistry* **1**, 923 (1962).
12. J. S. Griffith and L. E. Orgel, *Trans. Faraday Soc.* **53**, 601 (1957).
13. R. Freeman, G. R. Murray, R. E. Richards, *Proc. Roy. Soc. London Ser. A* **242**, 455 (1957).
14. H. M. McConnell and D. B. Chesnut, *J. Chem. Phys.* **28**, 107 (1958).
15. D. R. Eaton and W. D. Phillips, in *Advances in Magnetic Resonance*, J. S. Waugh, Ed. (Academic Press, New York, 1965), vol. 1, pp. 103-48.
16. D. W. Larsen and A. C. Wahl, *J. Chem. Phys.* **41**, 908 (1964).
17. G. N. La Mar, *ibid.*, p. 2992.
18. A. Kowalsky, *Biochemistry* **4**, 2382 (1965).
19. N. Muller and D. E. Pritchard, *J. Chem. Phys.* **31**, 768 (1959).
20. M. Karplus, *ibid.* **30**, 11 (1959); *J. Phys. Chem.* **64**, 1793 (1960).
21. H. J. C. Berendsen, *J. Chem. Phys.* **36**, 3297 (1962).
22. A. Saupe and G. Englert, *Phys. Rev. Letters* **11**, 462 (1963).
23. L. C. Snyder and E. W. Anderson, *J. Chem. Phys.* **42**, 3336 (1965).
24. R. C. Ferguson, *J. Polymer Sci. A* **2**, 4735 (1964).
25. F. A. Bovey and G. V. D. Tiers, *J. Polymer Sci.* **44**, 173 (1960).
26. C. W. Wilson, III, *J. Polymer Sci. A* **1**, 1305 (1963).
27. F. A. Bovey, F. P. Hood, III, E. W. Anderson, L. C. Snyder, *J. Chem. Phys.* **42**, 3900 (1965).
28. C. C. McDonald and W. D. Phillips, in *Proc. Conf. Magnetic Resonance in Biology 2nd* (Pergamon, New York, in press).
29. O. Jardetzky, N. G. Wade, J. J. Fischer, *Nature* **197**, 823 (1963).
30. E. W. Thomas, *Biochem. Biophys. Res. Comm.* **24**, 611 (1966).
31. C. C. McDonald, W. D. Phillips, J. Lazar, *J. Amer. Chem. Soc.*, in press.
32. A. Allerhand and H. S. Gutowsky, *J. Chem. Phys.* **41**, 2115 (1964); H. S. Gutowsky, R. L. Vold, E. J. Wells, *ibid.* **43**, 4107 (1965).

Antibody Variability

Somatic recombination between the elements of
"antibody gene pairs" may explain antibody variability.

O. Smithies

The amino acid sequences of polypeptides are uniquely controlled by the DNA of corresponding structural genes. Mutational events in the germ line alter these genes and lead to changes in the structure of polypeptides in later generations. A frequently observed result of mutations is the replacement of single amino acid residues, probably caused by single base-pair changes in the DNA (1). Less frequently the mutational events are more complex: a gene may be duplicated and subsequent divergent evolution may cause the descendants of the ancestral gene to code eventually for related but not identical polypeptides (2). Once a gene has been duplicated, triplications and higher orders of repetition arise relatively easily by unequal but homologous crossing-over between the duplicated genes (3). An unequal crossing-over between tandem duplicated genes can be represented as $2 \times 2 \rightarrow 3 + 1$ which correctly implies that the loss of the duplication is as likely as the reciprocal event, the formation of a triplication.

By extending these principles, one sees that multiple copies of related genes can arise but that they may be unstable in the germ line. Despite the potential instability of a multiple gene system, an obvious explanation of the variability of antibodies is that an animal carries in its genome a gene for every type of antibody polypeptide it may need. I will refer to this explanation of antibody variability as the *simple multiple-gene hypothesis*.

Lederberg (4) in 1959 proposed an alternative explanation that antibodies might be controlled by a small number of hypermutable genes. These hypermutable genes, transmitted regularly in the germ line, were presumed to undergo somatic mutation during the development of the immune system. I will refer to this as the *somatic mutation hypothesis*. The simplicity of the idea is appealing, and genetic mechanisms might be expected to have evolved to ensure that the needed hypermutability would be maintained and controlled. Lederberg in 1959 had little experimental informa-

tion on the types of variability actually existing in antibodies, and so did not propose any specific genetic mechanisms for obtaining hypermutability.

Experience with the genetic behavior of a partial gene duplication (Hp^2) in the haptoglobin system (5) led me, in 1963, to propose a mechanism that could permit antibody genes to be hypermutable in a genetically controlled way (6). I suggested that chromosomal rearrangements, caused by somatic crossing-over between duplicated regions of DNA in antibody genes, would lead to genetically predisposed variability. A specific model was considered requiring inversions within the antibody genes; it was compatible with the limited peptide data available at that time (see 7). The model was sufficiently specific that it could very easily be tested.

The major source of experimental data available at present on the nature of antibody variability is indirect. Natural antibodies produced by single cells can be detected, but their isolation and characterization is still impossible. Individually uniform monoclonal immunoglobulins are available only from humans (8) and mice (9) with multiple myeloma—a malignancy frequently leading to the production of large quantities of antibody-like proteins. These myeloma immunoglobulins consist of light and heavy polypeptide chains (10) and show serological types (8) similar to those observed in natural antibodies (11). The myeloma proteins are, however, much more homogenous.

Dr. Smithies is a professor of genetics and medical genetics at the University of Wisconsin, Madison. Portions of this material were presented at the Cold Spring Harbor Symposium on Quantitative Biology, 3 June 1967.